Mechanism of drag reduction by dimples on a sphere

Jin Choi, Woo-Pyung Jeon, and Haecheon Choi[a]
School of Mechanical and Aerospace Engineering, Seoul National University, Seoul 151-744, Korea

In this Letter we present a detailed mechanism of drag reduction by dimples on a sphere such as golf-ball dimples by measuring the streamwise velocity above the dimpled surface. Dimples cause local flow separation and trigger the shear layer instability along the separating shear layer, resulting in the generation of large turbulence intensity. With this increased turbulence, the flow reattaches to the sphere surface with a high momentum near the wall and overcomes a strong adverse pressure gradient formed in the rear sphere surface. As a result, dimples delay the main separation and reduce drag significantly. The present study suggests that generation of a separation bubble, i.e., a closed-loop streamline consisting of separation and reattachment, on a body surface is an important flow-control strategy for drag reduction on a bluff body such as the sphere and cylinder. © *2006 American Institute of Physics.* [DOI: 10.1063/1.2191848]

There are two most interesting flow phenomena about golf-ball dimples.[1] One is that dimples reduce drag on a sphere as much as 50% as compared to a smooth surface. The other is that the reduced drag coefficient, $C_D=D/(0.5\rho U_o^2 A)$, remains nearly constant over a range of Reynolds numbers, $Re=U_o d/\nu$, where D is the drag, U_o is the free-stream velocity, d is the diameter of the sphere, ρ is the density, ν is the kinematic viscosity, and A ($=\pi d^2/4$) is the cross-sectional area of the sphere.

The drag reduction by dimples has been explained such that dimples on a sphere induce a turbulent boundary layer on its surface and lower drag because turbulent boundary layer flow has a larger momentum than laminar boundary layer flow and thus delays separation. However, the detailed process of how dimples generate a turbulent boundary layer flow has not been fully investigated. To the best of the authors' knowledge, the only conjecture available in the literature was made by Bearman and Harvey,[1,2] who suggested that dimples generate discrete vortices energizing the boundary layer flow. However, no experimental measurement has been taken to prove this conjecture owing to the difficulty of measuring three-dimensional flow near dimples. Due to the same difficulty, the reason for a nearly constant drag coefficient over a range of Reynolds numbers, once it has been reduced, has not been explained yet. Again, the only conjecture made so far is that dimples fix the transition position far upstream at this Reynolds number range and thus keep a constant separation angle irrespective of the Reynolds number, resulting in a nearly constant drag coefficient.[1] However, the measurement supporting this conjecture has not been presented yet.

A nearly constant drag coefficient over a certain Reynolds number range was also found in the other types of surface modifications on a sphere. For example, Maxworthy[3] obtained this behavior of drag coefficient by placing a trip wire at a front-surface location. Nakamura and Tomonari[4] observed the same behavior by attaching a narrow roughness strip at a front-surface position. However, there was no discussion on the reason why the reduced drag coefficient remains nearly constant with these surface modifications.

Therefore, in the present study, we provide the mechanisms regarding to these two interesting phenomena: i.e., how dimples generate turbulence and why the reduced drag coefficient remains nearly constant over a range of Reynolds numbers. For this purpose, the drag on a sphere is directly measured using a load cell, the separation angle is measured from the surface oil flow pattern using a colored oil paint on a half-dimpled sphere, and for the first time the streamwise velocity above the dimpled sphere surface is measured using a hot-wire probe, respectively.

The present experimental setup consists of a sphere, supporter, load cell, traversing unit, and an open-type wind tunnel (the details on the experimental setup can be found in Jeon *et al.*[5]). A sphere of 150 mm diam is made of acryloni-
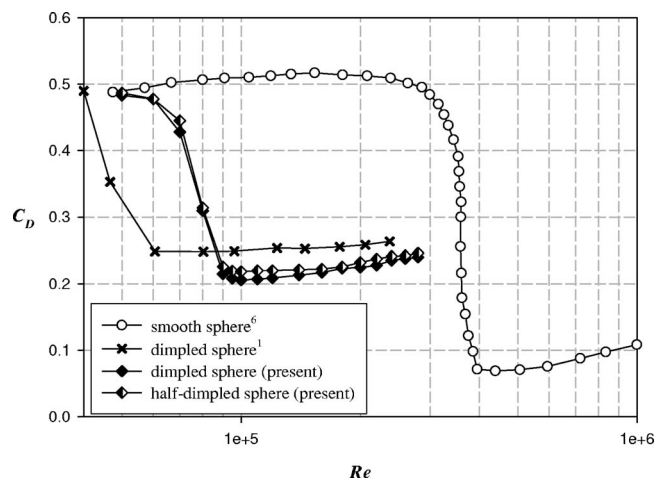

FIG. 1. Variations of the drag coefficient for smooth and dimpled spheres with the Reynolds number, together with the present result from a half-dimpled sphere.

[a] Also at National CRI Center for Turbulence and Flow Control Research, Institute of Advanced Machinery and Design, Seoul National University. Electronic mail: choi@snu.ac.kr
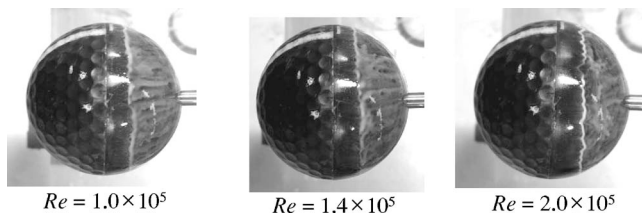
FIG. 2. Variation of the separation angle for a half-dimpled sphere with the Reynolds number. Shown in this figure is the oil flow pattern on the sphere surface. Oil is moved by the surface shear stress and thus is accumulated at the location of zero shear stress where the flow separation occurs. The separation angle is fixed at $\phi \approx 110°$ irrespective of the Reynolds number, where ϕ is the polar angle from the stagnation point. The flow is from left to right.

FIG. 3. Profiles of the time-averaged streamwise velocity (●) and rms streamwise velocity fluctuations (○) measured above dimples I–V: Re= (a) 1.0, (b) 1.5, and (c) 2.0×10^5. The angles in this figure denote the measurement locations. Also shown in (a) is the schematic diagram of spatial distribution of dimples I–V located at $\phi \approx 64° - 106°$ at which hot-wire measurements are conducted.

trile butadiene styrene (ABS) resin. The depth and surface diameter of dimples considered are 0.6 and 13 mm, respectively, and 392 dimples are almost uniformly distributed on the sphere surface. The present sphere with dimples is dynamically similar to a real golf ball (Titleist DT-Distance) without rotation. The free-stream velocity U_o varies from 5 to 28 m/s, corresponding to the Reynolds numbers of 0.5 $\times 10^5 - 2.8 \times 10^5$. At these Reynolds numbers, the flow above the smooth sphere maintains laminar boundary layer before the separation (82° from the stagnation point).[6] Therefore, unless some disturbances are introduced to the boundary layer, the flow keeps the laminar flow characteristics before the separation occurs.

Figure 1 shows the variations of drag coefficient for smooth and dimpled spheres with the Reynolds number. With increasing Reynolds number, the drag coefficient of the dimpled sphere shows a sharp decrease from that of the smooth sphere and then remains almost constant (but increases slowly). This results in more than a 50% drag reduction as compared to that of the smooth sphere. The Reynolds number range having a nearly constant drag coefficient depends on the depth, surface area, and the shape of the dimples. For example, the drag coefficient is nearly constant for Re $\geq 0.6 \times 10^5$ in Bearman and Harvey[1] ($k/d = 0.9 \times 10^{-2}$) but for Re $\geq 0.9 \times 10^5$ in the present study ($k/d = 0.4 \times 10^{-2}$). Here, k is the depth of the dimple. The drag coefficient of large k starts to decrease at a lower Reynolds number but has a higher constant value than that of small k, as shown in Fig. 1.

With the present dimples, the characteristics of boundary layer flow change significantly and the drag coefficient is reduced by more than 50% at Re $\geq 0.9 \times 10^5$ (Fig. 1). A nearly constant C_D irrespective of the Reynolds number is due to the fixed separation angle. To confirm this, we observe a surface oil flow pattern using a colored oil paint. However, the precise measurement of a separation angle using an oil paint is difficult[2,3] because oil movement is severely restricted by dimples. To avoid this difficulty, we use a half-dimpled sphere, i.e., dimpled on the front surface and smooth on the rear surface. This change in the rear-surface condition little modifies the flow characteristics over the dimpled sphere because C_D's for full- and half-dimpled spheres are nearly identical as shown in Fig. 1. Figure 2 shows the varia-
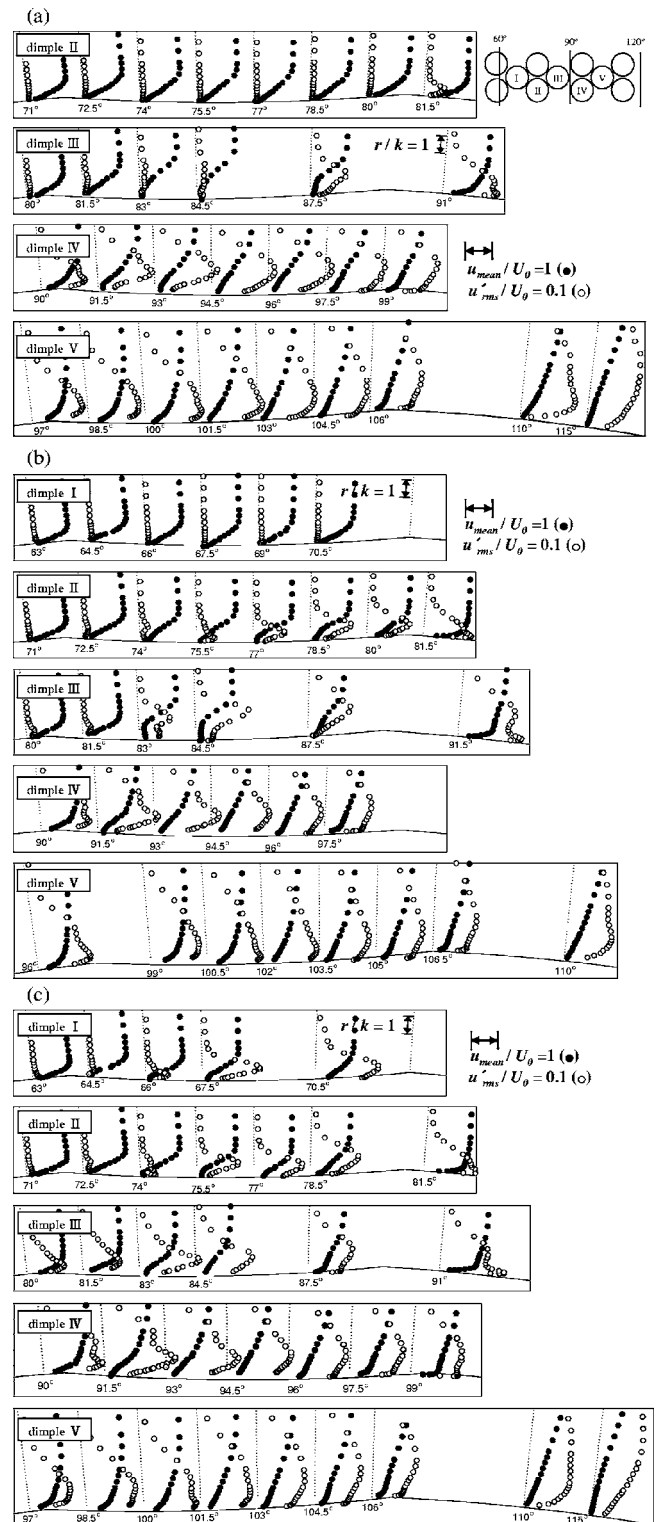
tion of the separation angle with the Reynolds number in the case of a half-dimpled sphere using a colored oil paint. One can clearly see that the separation angle is delayed and fixed at $\phi \approx 110°$ for different Reynolds numbers, agreeing well
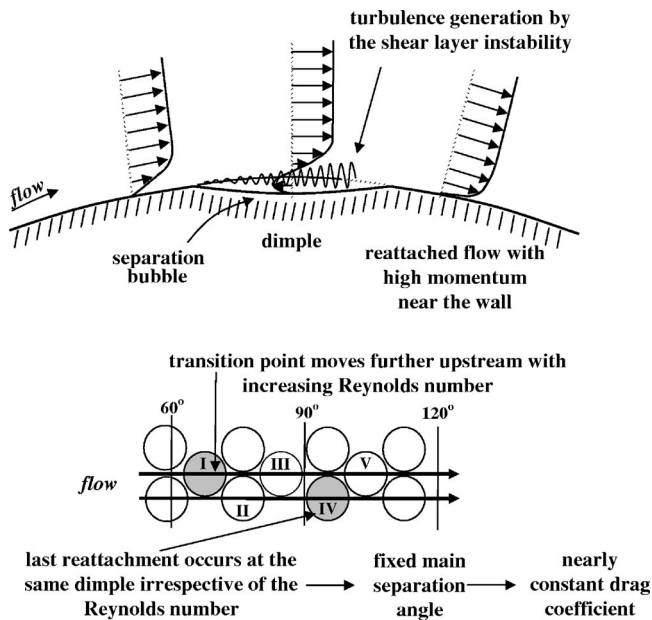
FIG. 4. Schematic diagram of drag-reduction mechanism by dimples.

FIG. 6. Energy spectra of the streamwise velocities measured at the radial location of maximum rms velocity fluctuations above dimple II ($\phi=78.5°$): $\cdots\cdots$, Re=0.5×10^5; ——, Re=1.5×10^5.

with the observation made in the relation between C_D and Re.

To investigate why the separation angle is delayed and fixed at $\phi\approx110°$ for Re$\geq0.9\times10^5$, we measure the streamwise velocity above the dimpled surface. Figure 3 shows the profiles of time-averaged streamwise velocity and root-mean-square (rms) streamwise velocity fluctuations above the dimpled surface. These profiles are taken along the centerlines of two rows of dimples. For Re=1.0×10^5 [Fig. 3(a)], the flow first separates at dimple III and the velocity fluctuations rapidly increase along the separating shear layer due to the shear layer instability (note that a flow separation is detected from the constant near-wall velocity profile along the radial direction when an type-I hot-wire probe is used). Then, owing to a significant increase in turbulence, the flow reattaches to the sphere surface and forms a separation bubble there. The reattached flow with high momentum near the wall overcomes the strong adverse pressure gradient formed in the rear sphere surface, resulting in separation delay. The last flow separation and reattachment occur at dimple IV. At dimple V, the flow does not separate because of high momentum near the wall. The main separation occurs after $\phi=110°$, resulting in a significant drag reduction. For Re=1.5×10^5 [Fig. 3(b)], the flow separates first at dimple II. Again one can observe a rapid increase in turbulence intensity above this dimple, which causes the flow to reattach on the surface with a high momentum near the wall and thus
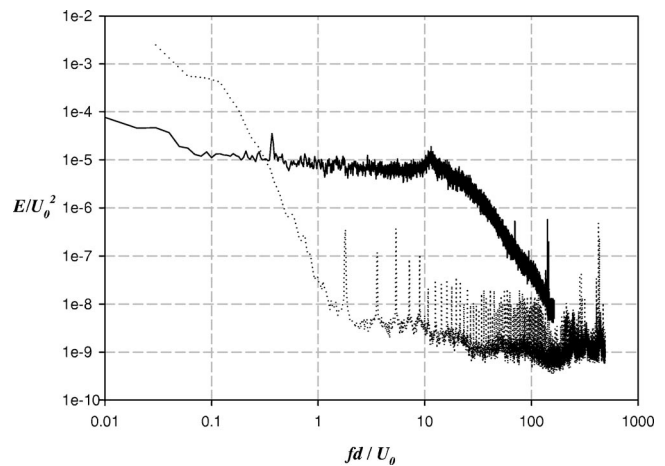
delays separation. The last separation and reattachment occur at dimple IV as for Re=1.0×10^5, and the main separation occurs after $\phi=110°$. For Re=2.0×10^5 [Fig. 3(c)], the flow separates first at dimple I, and last separation and reattachment occur at dimple IV. Therefore, with increasing Reynolds number, the transition position, where the flow receives energy from the shear layer instability after local separation, moves further upstream, but the last flow reattachment always occurs at the same dimple IV, which maintains a constant main-separation angle and drag coefficient for Re$\geq0.9\times10^5$. This mechanism of drag reduction by dimples is schematically drawn in Fig. 4.

Figure 5 shows the profiles of time-averaged streamwise velocity and rms streamwise velocity fluctuations above the dimpled surface for Re=0.5×10^5. At this Reynolds number, the present dimples do not reduce drag as shown in Fig. 1. The flow separates at dimple II and rms velocity fluctuations increase rapidly along the separating shear layer. The flow reattaches near the end of dimple II. However, as shown in the energy spectra in Fig. 6, the velocity fluctuations above this dimple have a high energy only at low frequencies due to low shear rates along the separation line, whereas the energy spectrum is broad-banded at the same location in the case of Re=1.5×10^5. Therefore, at Re=0.5×10^5, the reattached flow does not have sufficient momentum near the wall and thus cannot overcome the strong adverse pressure gradient there, resulting in no separation delay and no drag reduction. At dimple III, the flow separates completely (not shown here).

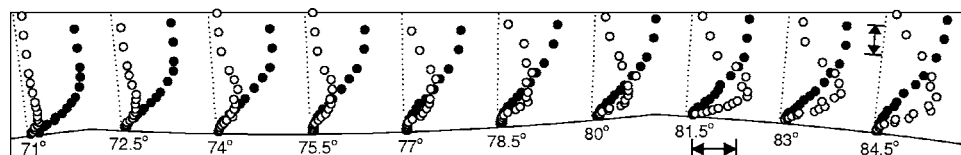In experiments of channel flow with dimples on one

FIG. 5. Profiles of the time-averaged streamwise velocity (●) and rms streamwise velocity fluctuations (○) measured above dimple II for Re=0.5×10^5. The horizontal and vertical arrows in this figure have the same meanings as those in Fig. 3.
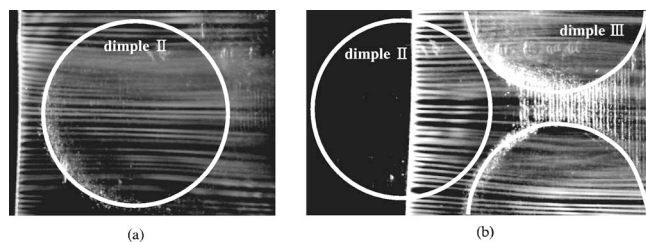
FIG. 7. Flow visualization above dimple II with a smoke wire at Re=1.5 ×10⁵. The smoke wire is located (a) just before and (b) in the middle of dimple II. The vertical white stripes appear in (b) due to the sphere surface condition: the original sphere surface had tiny grooves along the azimuthal direction because of the manufacturing process of the rapid prototype, but we made the sphere surface smooth by filling a transparent manicure into those grooves, which causes a light scattering from those grooves.

wall,[7,8] it was shown that vortex pairs are periodically ejected from the central part of each dimple and they increase turbulence transport there. To investigate the existence of such vortices even in the present flow, we perform a smoke-wire visualization very near the dimpled surface. Figure 7 shows the results of visualization at Re=1.5×10⁵. At this Reynolds number, the transition starts at dimple II [Fig. 3(b)]. Thus we locate a smoke wire of 40 μm diam inside the boundary layer as close to the surface as possible at two different places: just before and in the middle of dimple II. As is clear from Fig. 7, there are no such pair vortices above and right after dimple II. That is, in the present flow, the inception of transition to turbulence is not caused by such pair vortices. The existence of strong pair vortices found in Refs. 7 and 8 is owing to the choice of completely different ratios of the dimple surface diameter (L) to the boundary layer thickness (δ) and different incoming boundary layer flows from those in the present study: e.g., $L/\delta \approx 13$ and laminar boundary layer flow in the present study, whereas $L/\delta = 2$ and turbulent boundary layer flow in Ref. 8.

In the present study, we have shown that a very low drag coefficient of a dimpled sphere such as a golf ball results from the generation of separation bubbles inside dimples and the delay of separation through the shear layer instability. A similar mechanism was observed in the flow over a smooth sphere[9] when its drag coefficient becomes minimized (Fig. 1). Also, Jeon et al.[5] performed an active control on a smooth sphere for the purpose of drag reduction, and found that high-frequency blowing and suction generates a separation bubble near $\phi=110°$ and delays main separation to $\phi=130°$, resulting in a significant drag reduction. Furthermore, the variation of drag coefficient with the Reynolds number from the active control was nearly the same as that of the dimpled sphere. These previous studies strongly support the present mechanism of drag reduction by dimples. Finally, the present study suggests that generation of a separation bubble, i.e., a closed-loop streamline consisting of separation and reattachment, on a body surface is an important flow-control strategy for drag reduction on a bluff body such as the sphere and cylinder.

[1]P. W. Bearman and J. K. Harvey, "Golf ball aerodynamics," Aeronaut. Q. **27**, 112 (1976).
[2]P. W. Bearman and J. K. Harvey, "Control of circular cylinder flow by the use of dimples," AIAA J. **31**, 1753 (1993).
[3]T. Maxworthy, "Experiments on the flow around a sphere at high Reynolds numbers," J. Appl. Mech. **36**, 598 (1969).
[4]Y. Nakamura and Y. Tomonari, "The effects of surface roughness on the flow past circular cylinders at high Reynolds numbers," J. Fluid Mech. **123**, 363 (1982).
[5]S. Jeon, J. Choi, W.-P. Jeon, H. Choi, and J. Park, "Active control of flow over a sphere at a sub-critical Reynolds number," J. Fluid Mech. **517**, 113 (2004).
[6]E. Achenbach, "Experiments on the flow past spheres at very high Reynolds numbers," J. Fluid Mech. **54**, 565 (1972).
[7]P. M. Ligrani, J. L. Harrison, G. I. Mahmmod, and M. L. Hill, "Flow structure due to dimple depressions on a channel surface," Phys. Fluids **13**, 3442 (2001).
[8]S. Y. Won, Q. Zhang, and P. M. Ligrani, "Comparisons of flow structure above dimpled surfaces with different dimple depths in a channel," Phys. Fluids **17**, 045105 (2005).
[9]G. K. Suryanarayana and A. Prabhu, "Effect of natural ventilation on the boundary layer separation and near-wake vortex shedding characteristics of a sphere," Exp. Fluids **29**, 582 (2000).